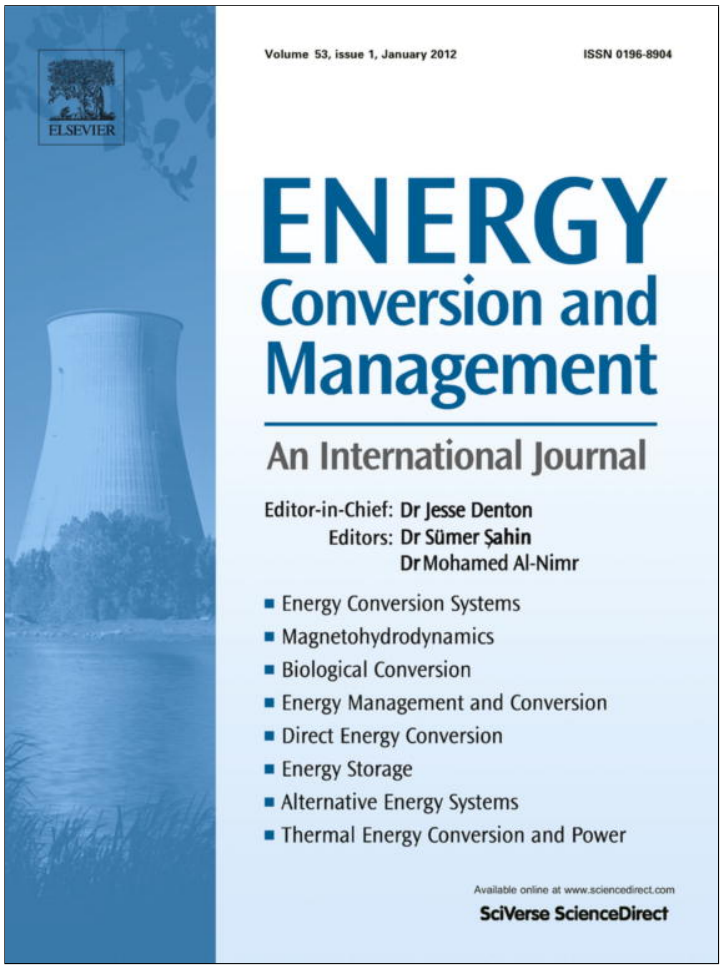

(This is a sample cover image for this issue. The actual cover is not yet available at this time.)

Energy Conversion and Management 62 (2012) 131–140

Contents lists available at SciVerse ScienceDirect

Energy Conversion and Management

journal homepage: www.elsevier.com/locate/enconman

Performance enhancement of photovoltaic array through string and central based MPPT system under non-uniform irradiance conditions

Syafaruddin [a,*], Engin Karatepe [b], Takashi Hiyama [c]

[a] Department of Electrical Engineering of Universitas Hasanuddin, 90245 Tamalanrea-Makassar, Indonesia
[b] Department of Electrical and Electronics Engineering, Ege University, 35100 Bornova-Izmir, Turkey
[c] Department of Computer Science and Electrical Engineering, Kumamoto University, 2-39-1 Kurokami, Kumamoto 860-8555, Japan

ARTICLE INFO

Article history:
Received 16 December 2010
Received in revised form 30 March 2012
Accepted 30 March 2012

Keywords:
Photovoltaic system
String MPPT system
Central MPPT system
RBF-ANN
Non-uniform irradiance

ABSTRACT

Mismatching losses reduction of photovoltaic (PV) array has been intensively discussed through the increasing penetration of residential and commercial PV systems. Many causes of mismatching losses have been identified and plenty of proposed methods to solve this problem have been recently proposed. This paper deals with reducing method of mismatching losses due to the non-uniform irradiance conditions. It is well-known that a certain number of multiple peaks occur on the power–voltage curve as the number of PV modules in one-string increases under non-uniform operating conditions. Since the conventional control method only drives the operating points of PV system to the local maxima close to open circuit voltage, only small portion of power can be extracted from the PV system. In this study, a radial basis function neural network (RBF-ANN) based intelligent control method is utilized to map the global operating voltage and non-irradiance operating condition in string and central based MPPT systems. The proposed method has been tested on 10×3 (2.2 kW), 15×3 (2.5 kW) and 20×3 (3.3 kW) of series–parallel PV array configuration under random-shaded and continuous-shaded patterns. The proposed method is compared with the ideal case and conventional method through a simple power–voltage curve of PV arrays. The simulation results show that there are significant increases of about 30–60% of the extracted power in one operating condition when the proposed method is able to shift the operating voltage of modules to their optimum voltages.

1. Introduction

Each individual cell composed PV module or each PV module composed PV array should be operated under the equal operating current and voltage in order to approach the ideal output power. In other words, the current–voltage (I–V) curves of modules must be similar. For instance, if a shadowed or damaged solar cell in a string causes that the cell produces current lower than the other cells then it will block the current flow from healthy cells to the output terminal of the string [1–3]. The generating current of solar cell depends strongly on irradiance level. In this reason, the effect of mismatch current is much worse than the mismatch voltage, the output power of PV module under this condition is remarkably reduced. This phenomenon is called as mismatching losses. Even the manufacturers set the tolerances in cell characteristic to reduce this kind of power losses; this problem continuously exists in the PV system practice. The causes of mismatching losses can be from the aging of solar cells, environmental stresses and shadow problems [4]. This problem urgently needs to be solved because of the increasing penetration of residential and commercial PV systems [5–8]. The reason is that the shadow condition can cause significant power losses in PV systems. Shading in one single cell inside the PV modules can result in 90% of total power losses. Further problem is that the optimum point of PV array under the partially shaded condition is shifting far from the local maxima where the conventional controller is used to be operated. For this reason, the researchers have concentrated to develop the robust MPPT controllers to overcome the mismatching losses.

The state of technique for the PV inverters has been matters of concern for the application of PV system below and above 10 kW including inverter topology [9,10]. On the other hand, finding the state of art of different control approaches for the parallel inverter operation is not easy right now since there are many proposed control strategies in the literature [11,12]. One idea to solve the mismatching losses in PV system practice is to provide module, string and central based MPPT configurations. Module based system can be defined as an individual MPPT connected to each PV module. This type of configuration seems very reliable since the equipments can be easily replaced once they get broken without affecting the remained parts. Normally, this kind of system connection is suitable when the PV size is small. However, when the

* Corresponding author.
E-mail address: syafaruddin@unhas.ac.id (Syafaruddin).

0196-8904/$ - see front matter © 2012 Elsevier Ltd. All rights reserved.
http://dx.doi.org/10.1016/j.enconman.2012.03.028

capacity of PV system increases denoted with high number of modules, the module based system becomes less proper due to complicated wire connection, hard maintenance and high installation cost. In addition, the module based system is facing some problems, such as the existing devices often suffer from high cost or poor efficiency, the maintenance procedures would be quite complex, which is comparable to the one of PV modules. Another constraint is that module based system have practically the same requirements to grid compatibility, such as safety, harmonics, electromagnetic compatibility as traditional inverters [13]. Although the module based MPPT system may produce much higher output power under partially shaded conditions [14], the module based system might cause excessive complexity due to the mentioned reasons. Therefore it is not further discussed in this paper.

The interesting point to be discussed is actually comparing the performance between string and central based MPPT system configurations. He et al. [15] proposed a method to evaluate and optimize inverter configurations for grid-connected PV systems. String based system means that a single MPPT unit is connected to one string of PV array. For instance 10×3, 15×3 and 20×3 PV array, it requires three units. On the other hand, the central based system means a single unit handles the power conditioning of the whole PV array. It is difficult to say that the central configuration is much better than the string or vice versa, since there are various possible unpredictable shading conditions and different sizes of PV array. In Ref. [16], modified central and string inverter configurations are proposed, that result in considerable reduction in partial shading losses. Villarejo et al. [17] compares the performance ratio of PV plants using central and distributed inverters by using a single diode model. They developed a graphical method to estimate the power generation under different solar irradiation and temperature conditions. On the other hand, Deline [18] analyzed the impact of partial shading conditions on multi-string PV system with and without dc–dc converters with several different system assumptions needed in this simulation analysis. In Ref. [19], the mismatch losses and the power losses due to failure in tracking of the global maximum power point of a long string of 18 series-connected PV modules and three short strings of six series-connected PV modules connected in parallel are investigated under different partial shading conditions using MATLAB–Simulink simulation model. Foiadelli et al. [20] evaluate modular, string and central based topologies for grid connected PV plant by analyzing the problem of the currents drawn to ground for the effect of the switching of the various converters, basing on a EMTP–ATP dynamic simulation tool. As results, it has been suggested that different configurations and operation strategies should be further studied and tested in order to reduce the mismatch losses, which is similar to the conclusion in Ref. [15].

In addition, the financial concerns are still very important for PV system. Intuitively, the multiple inverters will have lower energy losses in associated with partial shading in string based system. Nevertheless, a tendency of several commercial inverters under string configuration behaves worse under partial shading [21]. From the investment point of views, the cost of three units of medium size inverter is almost same with the cost of one single big size of inverter. However, the gain from mismatched reduction is not enough to compensate for the additional cost of string inverter installations when the PV size less than 5 kW. Therefore, a central inverter is always chosen in the UK for the PV system < 5 kW [22]. Beyond these achievements, the central based system show a number of drawbacks, such as the necessity of high DC cables between the PV array and the inverter, reduced efficiency due to mutual influence of PV module and extra diodes in each string and as well as the difficulty in gradual expansion of the system capacity [23]. From these reasons, the string based system is still the promising option for the sake of the reinforced system reliability and reducing the mismatched problem under partially shaded condition. Nevertheless, the optimum size of inverter should be determined in the simpler proper method due to several aspects play important roles in the grid-connected PV application [24].

This paper contributes the solving mismatching problems by observing the performance of string and central based systems accompanied with intelligent control method for different sized PV arrays under various non-uniform irradiance conditions. In fact, the inverter efficiency is highly affected by the irradiance profiles entering the PV modules surface [25,26]. Under such conditions, as the number of PV modules increase in one string, there will be multiple peaks observed in the power–voltage (P–V) curve. Since the tracking process of conventional controllers start from the open circuit voltage, the tracking process is oscillating around the first local maxima close to the open circuit voltage (V_{oc}) point and they are not smart enough to reach the global MPP. As a result, the conventional controller is totally failed to find the global peak which causes the output power cannot be maximally generated. In addition, there are several proposed MPPT controllers when integrated with the inverter operation; they will not bring optimal utilization to the overall grid performance [27]. To solve the problem, this study comes up with the intelligent based control method by implementing radial basis function neural network to estimate the optimum operating voltage. This method is directly localized the optimum point without any stepping process wherever the irradiance conditions are changed; therefore the tracking process is fast and simple. Moreover, the training process of this method is less time-consuming even in the case of multiple strings after upgrading the size of PV array. To reach the objective of this proposed method, the optimum voltage is used as the reference signal for the MPPT controller. It was demonstrated in [28], once the optimum voltage at the global peak can be determined in time and used as the reference for the controller, it ensures that the PV system can operate at the global MPP. Two scenarios called random-shaded and continuous-shaded patterns were tested in 10×3 (2.2 kW), 15×3 (2.5 kW) and 20×3 (3.3 kW) of series–parallel (SP) PV array configurations. The results are showing promising high percentage of 30–60% of extracted output power in compared with conventional controller method. This result is significantly notified when the PV size increases.

2. PV system configuration

The PV system is conventionally structured by connecting the PV array to the power conditioning unit (PCU) before utilizing the output power to the grid. The PV array itself can be constructed in different configurations, such as series–parallel (SP), bridge-link (BL) and total cross tied (TCT) [29]. In this study, the PV array consists of 10×3 (2.2 kW), 15×3 (2.5 kW) and 20×3 (3.3 kW) of series–parallel connected PV array. Each PCU is responsible for the power conditioning of PV array where they are connected. In Fig. 1, the proposed string and central MPPT units based PV system configurations are presented. The ideal dc–dc converter is used to force the three PV arrays in operating at the MPP [30]. In the left hand side of this figure, the RBF-ANN (1) is utilized to generate the optimum voltage of each string for dc–dc converter. The optimum voltage for the first, second and third string of PV array is denoted by V^*_{s1}, V^*_{s2} and V^*_{s3}, respectively. On the right hand side, the RBF-ANN (2) is utilized to generate the optimum voltage of PV array, which is specified as V^*_c. To observe the performance of the proposed systems under non-uniform operating conditions, different size of PV array are considered by using SM-55 PV module [31]. The local and global MPP points are taken into consideration when investigating performance of the proposed system for string and central based MPPT schemes.

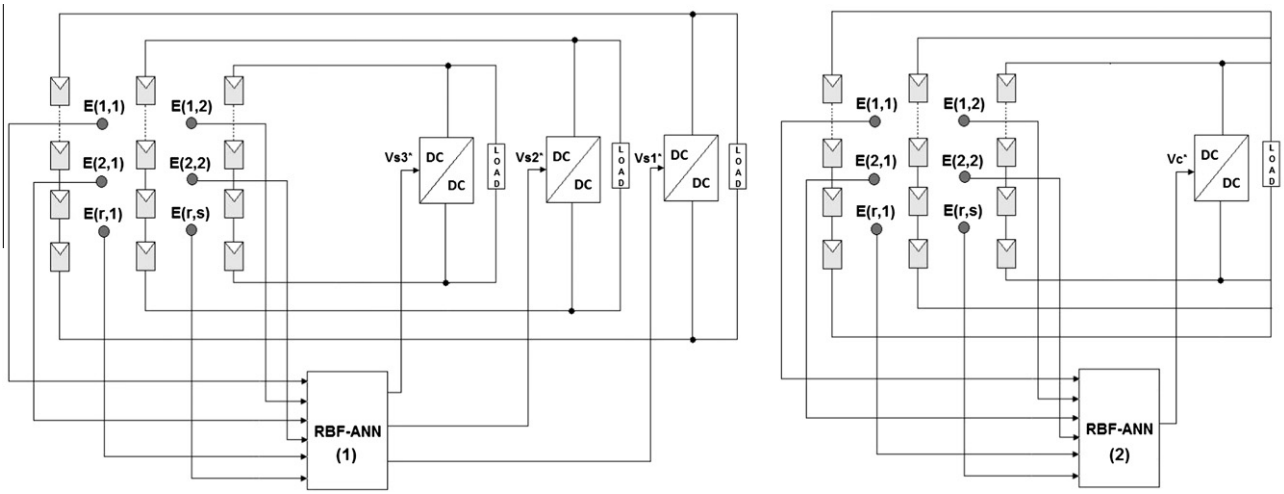

Fig. 1. The proposed string and central based PV system configuration.

Field testing is costly and time-consuming process and it depends heavily on prevailing weather condition. In addition, it is very difficult to supply identical operating conditions when comparing the performance of string and central based MPPT systems. For these reasons, the circuit-based simulation model is very important to provide properly the inclusion of mismatch effects with high accuracy [32,33]. In this study, non-uniform operating conditions are generated randomly under Matlab/Simulink environment for 10×3, 15×3 and 20×3 PV array. One of typical operating conditions for PV arrays is shown in Fig. 2. As shown in the figure, the value indicates the irradiance level in W/m^2 on each module. Due the nature characteristic of the bypass diode connected in the module, there will be multiple peaks occur in the *P–V* curve. Consequently, the global optimum point may be shifting in wide range of voltage window from open circuit voltage. Under this condition, the global MPP and local MPP close to open circuit voltage are given for string and central based PV configurations as shown in Tables 1 and 2, respectively. For the string based configuration, much more output power can be generated under this operating condition when the controller is able to reach the global MPP point than for those controllers which are only operated at the local MPP point close to open circuit voltage. The same condition occurs in central inverter as appeared in Table 2. The important result for these two measurements is that the output power can be generated much higher when the controller can be operated at the global MPP point of each string base of PV array. This point is challenging and should be further explored.

Table 1
Global and local MPP for string based PV array under the given conditions in Fig. 2.

PV array	String-1		String-2		String-3	
	At global MPP					
	V_m (V)	P_m (W)	V_m (V)	P_m (W)	V_m (V)	P_m (W)
10×3	125.01	211.20	109.68	244.43	120.81	92.72
15×3	191.50	290.85	190.33	241.83	245.29	304.74
20×3	276.10	440.59	166.09	238.23	219.62	330.56
PV array	At local MPP nearest to open circuit voltage					
10×3	174.21	68.02	174.22	149.30	160.34	56.95
15×3	257.65	101.20	249.84	203.46	245.29	304.74
20×3	358.52	130.14	334.82	113.07	350.90	130.92

Table 2
Global and local MPP for central based PV array under the given conditions in Fig. 2.

PV array	Central based MPPT system			
	At global MPP		At local MPP	
	V_m (V)	P_m (W)	V_m (V)	P_m (W)
10×3	113.06	525.87	164.90	272.89
15×3	192.99	805.09	246.56	606.41
20×3	257.43	980.50	350.90	372.02

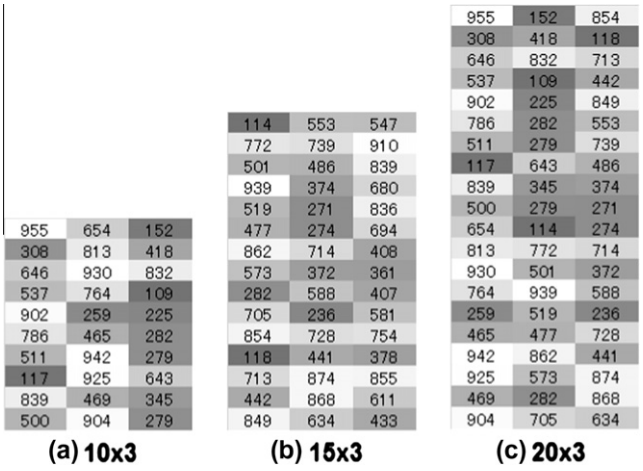

Fig. 2. A typical heavily shaded irradiance conditions for three different sized PV arrays.

The proposed method is intended to find the global MPPs under the non-uniform operating conditions. This is very difficult for classical MPPT controllers [3,34]. In this reason, an intelligent technique is required [1]. For this task, radial basis function (RBF) neural network is utilized in this study. The RBF neural network is well-recognized with fast training process with high accuracy estimation. The purpose of this method is to estimate the voltages of string and central based system that correlates to the global maximum power point. Since the conventional controller is commonly started from the open circuit voltage, it is almost impossible to reach the global peak due to the step time operation. For this reason, the intelligent technique based control system is the promising solution because the controlling method able to find the global peak in time directly without doing any iteration process; therefore it is fast to be implemented in the real-time application [35]. The only procedure to establish the controller is to set the training data for training process in each target case. In this paper,

the training data set is the estimated optimum voltage as the function of modified input irradiance on each PV array. This approach is taken following the assumption that once the global optimum voltage is reached and the global peak power [28]. The details about the selection of input–output data set, the training process and the validation process will be explained in the next section.

3. Radial basis function (RBF)-ANN based optimum voltage

The artificial neural network is successfully compatible with the optimization problem of PV system [36,37]. It is due to the nature characteristic of PV system as a non-linear system. Solving the non-linear characteristic of PV system with conventional optimization techniques or other numerical methods may require particular computational techniques, time consuming and difficulty in convergence stage [38]. Another characteristic output of PV systems is their intermittency outputs due the environmental factors. The output power of PV system is really affected by the irradiance level and ambient temperature following the nature characteristic of photocurrent [39]. Therefore, tracking the optimum operating point is necessary in order to reach the maximum efficiency conversion of PV system. In some MPPT controllers as explained in [28,40,41]; the optimum voltage as reference controller is very important. However, the operating voltage is influenced by temperature. If the temperature increases, the voltage is reduced or vice versa. Moreover, under partially shaded or mismatched cell condition, the optimum voltage may reduce significantly from its optimum point. To overcome such kind of problems, an intelligent technique by means the artificial neural network is the promising solution to identify the optimum points under any scenarios [42–45].

In this study, the variant of ANN methods called radial basis function (RBF) neural network is utilized as controller to estimate the global MPP voltage of each string PV array. This method is well-recognizable fast during the training process, the network structure is directly confirmed after training and it has high accuracy during the validation [46]. RBF neural network is a typical neural network structure using local mapping instead of global mapping as in multi layer perceptron (MLP) [47]. In MLP method, all inputs cause an output, while in RBF method; only inputs near a receptive field produce activation function. The hidden layer is locally tuned neurons centered over receptive fields. Receptive fields are located in the input space areas where input vectors exist. If an input vector lies near the center of a receptive field, then that hidden layer will be activated. Because of this approach, the training process using RBF network is very simple. Once the set goal error is reached, the training is stop and the number of hidden nodes is confirmed. For utilizing this technique, only training process is required and after the structure is confirmed; the network may respond well to different operating conditions. In general, the stage in the RBF method consists of training data set selection, training process and validation process; and all these stages will be explained as follows.

The input signal is the modified irradiance level which is randomly generated. The random data is considered to follow the nature characteristic of irradiance level arriving on the module. The modified irradiance means that one sensor measures the average of four adjacent modules [40]. This method is proven sufficiently to limit the data variation that makes the convergence easier during the RBF training process. Also, the computational burden can be released as the number of input nodes decrease. In this study, the output signals are the estimated MPP voltage on each string called V^*_{s1}, V^*_{s2} and V^*_{s3}. On the other hand, only V^*_c is the output of estimated MPP voltage for central based MPPT unit.

The approach to determine the input signal is explained as follows. Let assume the size of PV array is $A(m,n)$ and the irradiance arrives on each module is $E_{A(m,n)}$; the average irradiance on four adjacent PV module $E(r,s)$ as the input signal can be calculated as:

$$E(r,s) = 0.25x[E_{A(r,s)} + E_{A(r,s+1)} + E_{A(r+1,s)} + E_{A(r+1,s+1)}] \quad \text{for } r = 1,2,3,\ldots,m-1 \quad \text{and} \quad s = 1,2,3,\ldots,n-1 \tag{1}$$

Using this approach, the input signal can be generated with dimension 18, 28 and 38 inputs, instead of 30, 45 and 60 inputs for 10×3, 15×3 and 20×3 PV array, respectively. Under any input signal conditions, $E(r,s)$, the global MPP voltage refers to the ideal case. A number of data set patterns are prepared for this purpose and this approach is legitimately implemented to both string and central based MPPT unit assessment.

The second stage is the training process. During the training process, the input vector which will result in lowering the network error is used to create a new hidden neuron. If the current error after the neuron insertion is low enough, the training stops. In this study, the parameter of training process: the mean squared error goal (GOAL), spread of radial basis functions (SPREAD), maximum number of neurons (MN) and the number of neurons to add between displays (DF) are 0.003, 1.0, 25, 1, respectively. The outcomes of the training process are the number of the hidden neurons that represent the structure of RBF neural network and the training error that represents the accuracy of the confirmed structure. As results, for string based MPPT unit, there are 23, 22 and 23 of hidden neurons and 0.0003775, 0.000973 and 0.001714 of training errors for RBF structure of 10×3, 15×3 and 20×3 PV array, respectively. Meanwhile for central based MPPT unit, the number of hidden neurons (training error) for 10×3, 15×3, and 20×3 PV array are 34 (0.0004662), 32 (0.0008256) and 35 (0.0009264), respectively. It seems in these results that simpler structure is obtained for 15×3 PV array than other sizes for both MPPT units assessment. It is due to merely the simplicity correlation between the input data and the target output and the data cannot be forced to convergence in the same structure because their random nature.

At glance, the RBF structure as shown in Fig. 3 is similar to the three layered feed-forward neural (TFFN) network in terms of weights and biases connection between layers. Fig. 3a and b represent the RBF-ANN (1) and RBF-ANN (2), respectively. The weights w_1 connect the input layer to the hidden neurons and weights w_2 connect the hidden neurons to the output layer. Also, there are two biases b_1 and b_2 for utilizing this network. The only different is the implementation of transfer function between layers. In TFFN structure, the sigmoid function is the common utilized activation function in all layers, but this consideration is also case by case depending on the target of study and the complexity input–output data patterns. In RBF network, in the first layer, the Euclidean distance weight function is applied for all input signals and its connected weight w_1 and bias b_1, before preceding them to the '*radbas*' activation function. This algorithm can be formulated as follows:

$$a_1(n) = radbas \quad [dist\ (w_1(n,1)E(1,1) + w_1(n,2)E(1,2) + \ldots..w_1(n,r)\ E(1,r)).\ b_1(n,1)] \tag{2}$$

where n is the nodes number of hidden layer. In the string based structure, n is equal to 23, 22 and 23 for 10×3, 15×3 and 20×3 PV array, respectively. Meanwhile, in the central based structure n equals to 34, 32 and 35 for 10×3, 15×3 and 20×3 PV array, respectively. In addition, r is the number of input signals where r is equal to 18, 28 and 38 for 10×3, 15×3 and 20×3 PV array, respectively.

After this process, the output layer a_2 is calculated by simply applying the '*purelin*' activation function between a_1 and weights w_2, include the bias b_2 of the second layer. The mathematical model is stated for this condition as:

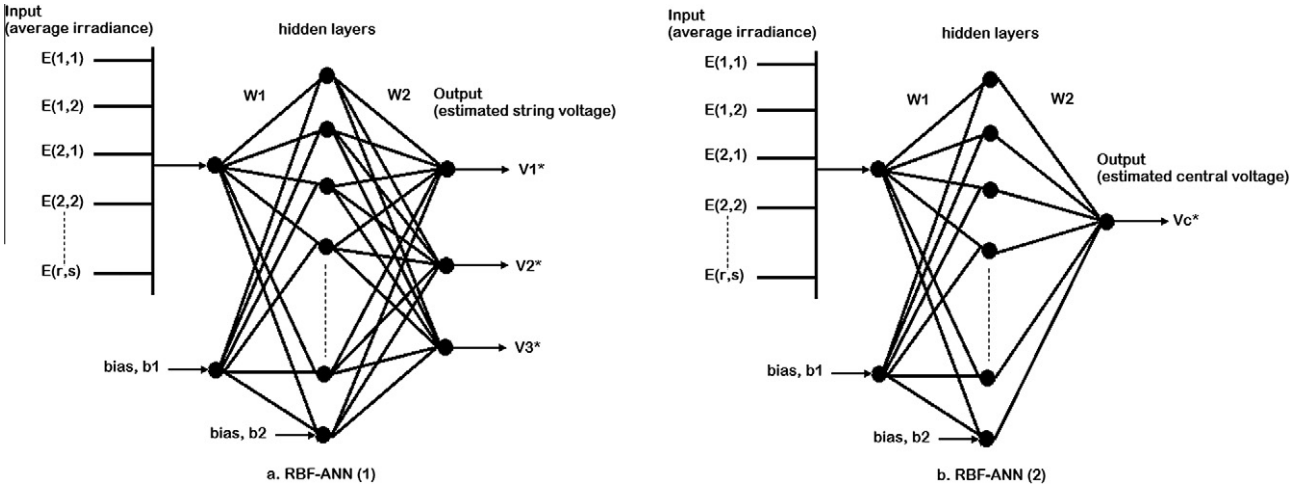

Fig. 3. The proposed RBF-ANN structure for string and central based MPPT systems.

$$a_2(m) = purelin\left[\left(\sum_{n=1}^{n} w_2(m,n).a_1(n)\right) + b_2\right] \quad (3)$$

where m is the nodes number of the output layer. In this case, m equals to 3 and 1 for string and central based MPPT units, respectively for all sizes of PV array.

The last stage of construction the RBF network is the validation process where the proposed structure is tested with different input signals other than data used in the training process. The purpose of this stage is to evaluate the accuracy of network to respond in different signals conditions. Again, the test validation data is also randomly generated. One of the typical irradiance levels for such testing of 10×3, 15×3 and 20×3 PV array is shown in Fig. 4. In this figure, the irradiance profile on each module is totally different each other. In the string based system, the multiple peaks occur and the global MPP point may be far away from the local maxima. A similar trend of global MPP point is possibly found under central based system measurement.

The accuracy of the estimation process through the RBF method is provided in P–V curve depicted in Fig. 5. The investigation is focused on the P–V curve measurement on string basis. The estimated point is denoted with asterisk sign (G^*), while for those without asterisk (G) is the target value. The estimation result by this method is not exactly reach the global point (the ideal case), but it is able to reach the second peak close to the global peak. Since the second peak power not so far from the global MPP point, the estimation can be successfully considered using the proposed method. This might be better than other conventional techniques on string basis which only able to operate close the local maxima (L). For instance, In Fig. 5a, the $G1^*$, $G2^*$ and $G3^*$ are very close to points $G1$, $G2$ and $G3$, respectively in 10×3 PV array. This approach yields output power 37% higher than using conventional controller on string basis. Almost the same outcomes for 15×3 PV array in Fig. 5b and this yields 36.8% than controllers operated in the local maxima on string basis. A significant extracted output power of about 54.7% is reached for 20×3 PV array (Fig. 5c). In these figures, the estimation MPP based central MPPT is also provided for different PV array sizes. The accumulation output power using string based MPPT is consecutively higher than that of central based MPPT unit measurement. Based on this verification, the proposed method by means the string based MPPT unit can adapt to the heavily shaded patterns with reasonable accuracy. To convince the robustness of this method; wide different scenarios will be tested using this method.

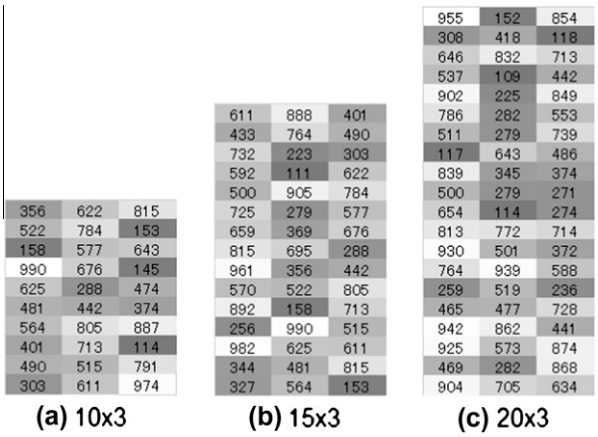

Fig. 4. A typical heavily shaded patterns used for the validation process.

4. Simulation results

To ensure the proposed method, two scenarios of irradiance pattern have been demonstrated. They are the random shaded pattern and the continuous shaded pattern. Again, these conditions can be randomly generated.

4.1. Random shaded pattern

The random shaded patterns are shown in Fig. 6. This pattern is generated taking the assumption that irradiance level on each module is different and non-regularly distributed. Fig. 6a, b and c represent the input signal under this scenario for 10×3, 15×3 and 20×3 PV array, respectively. Also, the pattern can be generated as the incremental time for the assumption that this kind of input can be continuously appeared during the daily operation of PV system. In this study, the definite time for the data irradiance is specified at $t = t1$, $t = t1 + 1$ and $t = t1 + 2$. Under this condition, the performance of the proposed method is compared to the ideal condition using central and string based system and the condition where the controllers operate in the local maxima close to the open circuit of PV array. The change in output power with respect to the ideal case which is represented by ΔP (in percentage), is defined as:

$$\Delta P = \frac{P_{proposed} - P_x}{P_{proposed}} \times 100\% \quad (4)$$

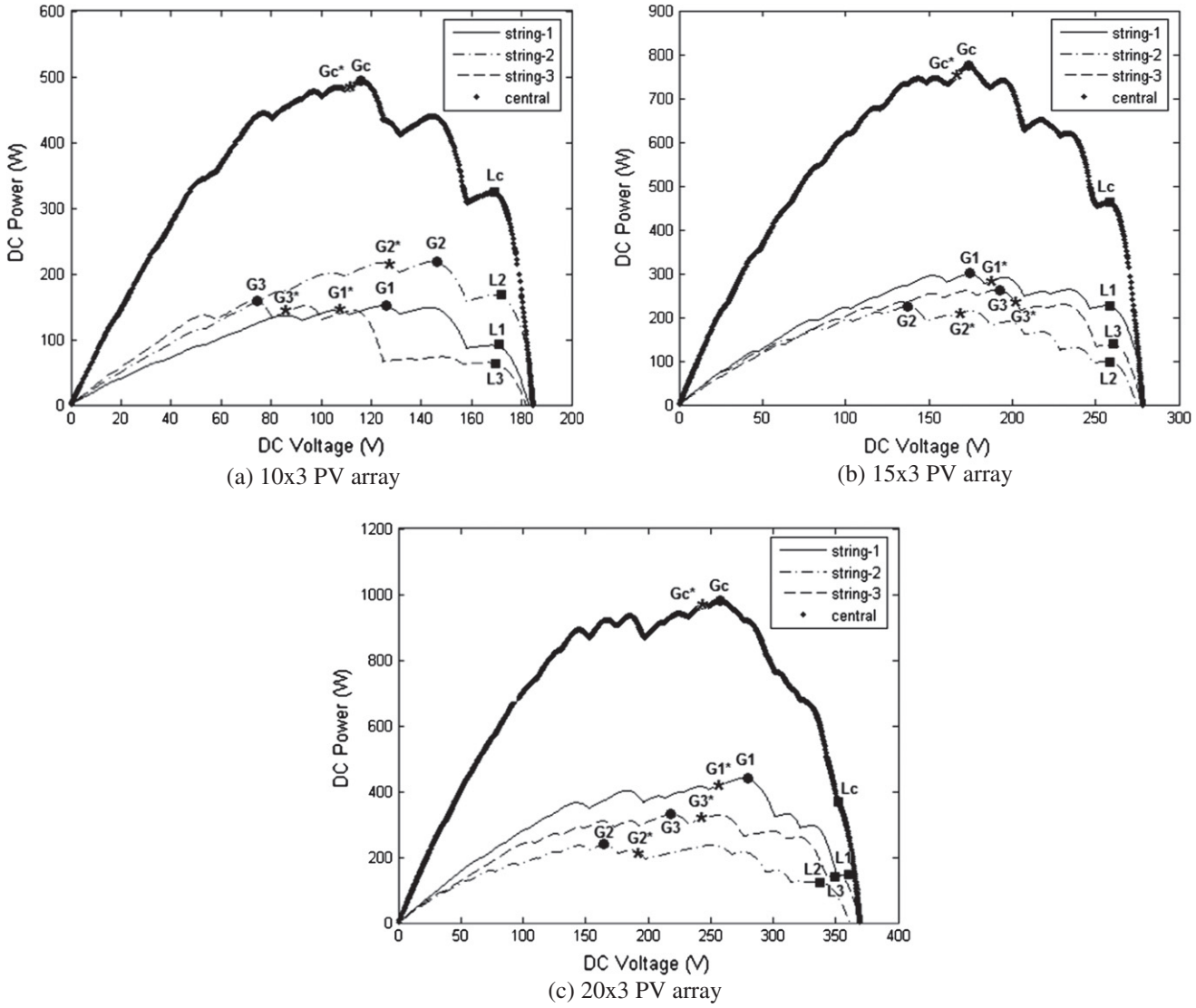

Fig. 5. The estimated, global and local MPPs on string and central based PV systems.

where P_x may represent the power at ideal condition for Table 3 measurement and power at the local maximum point for Table 4 measurement.

The comparison results as shown in Tables 3 and 4 are in terms of the percentage of extracted output power. As shown in Table 3, the output power yields using the proposed method are generally lower that the output power yields based on the ideal condition for both central and string based system. To the central based MPPT PV array, small increment of output power can be produced as the time goes on for 10×3 and 15×3 PV array; but this trend does not work out for 20×3 PV array. However, even like that the decreasing output is not more than 7% for $t = t1 + 1$ in 20×3 PV array. Similar trend of lower output power than the ideal case is obtained for string based MPPT unit. This trend is clearly depicted in Table 3 for all sizes of PV array. Under this scenario, the output power is totally lower at the beginning of simulation; then little improvement is obtained for 10×3 and 15×3 PV array. These outcomes conversely occur in the 20×3 PV array. The negative signs indicate the output power from both string and central based MPPT units is lower than the ideal output power that is supposed to be. Such outcomes are reasonable since it is difficult to have MPPT system that is working similar to the ideal case.

The benefits of this method can be seen in the results shown in Table 4 when the output power from the proposed method is compared with the performance of conventional controller in central and string based system. There are significant of 29.31–62.73% of incremental output power when compared with conventional controller in the central based system. The average contribution is about 42.63%, 49.07% and 47.79% for 10×3, 15×3 and 20×3 PV array, respectively. Again, since the proposed controller is in the string basis, little lower output power from the proposed method is obtained than the central case. The incremental output power is in the range between 28.43–61.80%. From this view point of both case comparisons, significant output power/energy can be yielded using the proposed method for the long term performance of PV system, like one-day or one year operation if the heavily shaded conditions persist.

4.2. Continuous shaded patterns

The proposed method is also tested with another typical shade patterns called continuous-shaded patterns as shown in Fig. 7. In compared with the previous case, the shading pattern is more regular from one side of the module to other sides. In this case, the

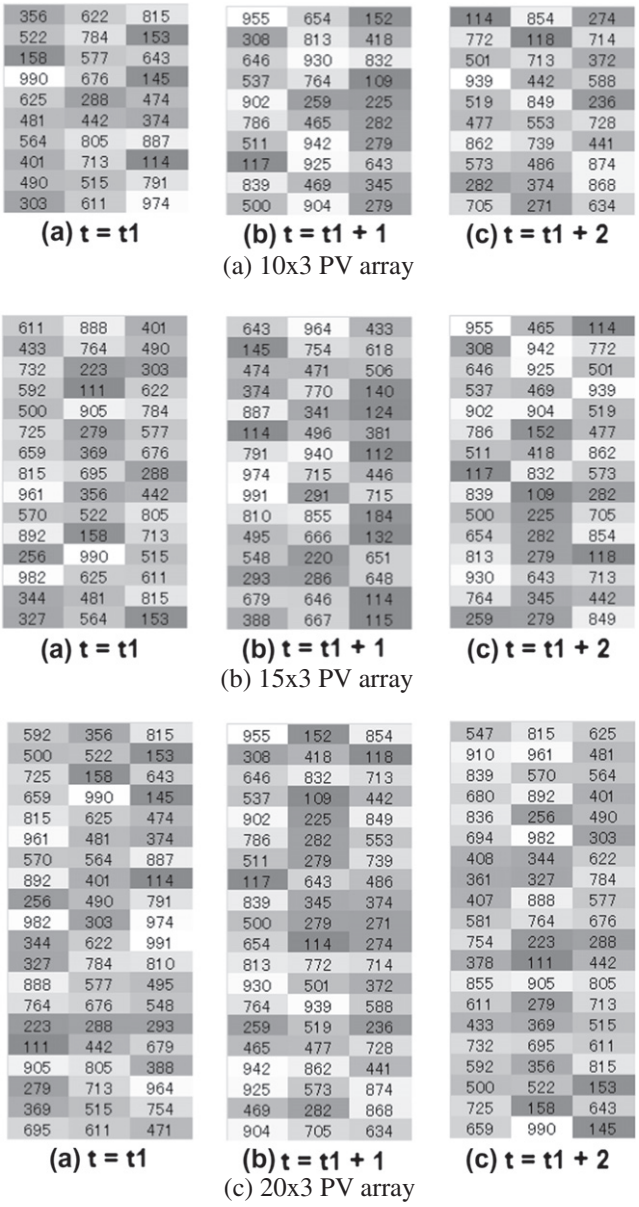

Fig. 6. Random shaded patterns for three different sized PV arrays.

Table 3
Percentage of extracted power of proposed method in compared to the ideal condition.

PV array	ΔP (%)					
	String based MPPT			Central based MPPT		
	$t = t1$	$t = t1+1$	$t = t1+2$	$t = t1$	$t = t1+1$	$t = t1+2$
10 x 3	−11.68	−0.14	−0.21	−3.68	−3.97	−2.44
15 x 3	−7.75	−3.19	−0.08	−5.63	−3.80	−0.05
20 x 3	−4.66	−9.93	−8.18	−2.1	−6.79	−3.66

Table 4
Percentage of extracted power of proposed method in compared to the local maxima.

PV array	ΔP(%)					
	String based MPPT			Central based MPPT		
	$t = t1$	$t = t1+1$	$t = t1+2$	$t = t1$	$t = t1+1$	$t = t1+2$
10 x 3	31.78	47.85	31.78	47.85	31.78	47.85
15 x 3	36.80	42.50	36.80	42.50	36.80	42.50
20 x 3	54.66	55.61	54.66	55.61	54.66	55.61

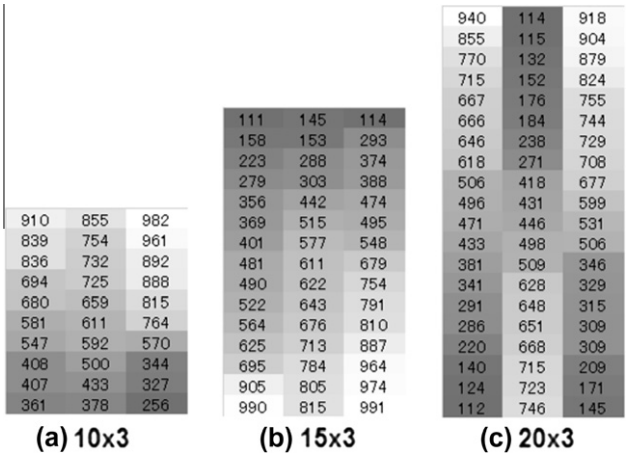

Fig. 7. Continuous shaded patterns for three different sized PV arrays.

irradiance level is gradually degrading that cause continuous patterns. There are three conditions provided in this test. For 10×3 PV array, the shading pattern is from top of the module (positive terminal) to the bottom part (negative terminal). This shading pattern is oppositely set in the 15×3 PV array. A little different shading pattern is set for 20×3 PV array where the first and third strings are shaded in the negative terminal, while the second string in opposite way. The optimum voltage identification is provided form this proposed method in compared to the ideal and local maxima case.

It can be seen in Table 5 that the proposed method can respond well to the different input conditions. Actually, this achievement was previously predicted that if the proposed method can respond to the random shaded patterns, it is highly recommended working under the continuous shaded patterns. It is due to the capability of the proposed method respond to the generated random operating conditions. In this result, for instance the 10×3 PV array, the global MPP voltage V2 of the second string is shifting to 88.99 V in the ideal case, the proposed method can achieve 79.10 V instead of 171.29 V in the local maxima. As results, the output power P2 can be approached very close to the ideal case. Also, high accuracy is shown for the estimation of voltage in strings 1 and 3. On the other hand, when shaded pattern condition follows the 15×3 PV array, the global MPP voltage of all strings is shifting far from the local maxima. But, again the proposed RBF method can reach very close to expected values in the ideal case. The same achievement is obtained for 20×3 PV array under the defined continuous shaded patterns. Also, the output power accumulation from string based MPPT unit is noticeable higher than the one from the central based MPPT unit output. Based on the results showing in different scenarios, the RBF method is robust to estimate the voltage on string basis and this estimation makes the output power is increasing very significant.

5. Discussion

In the future, a significant number of PV systems will be installed not only on the roofs but also wherever sunlight is available. It is crucial to improve the efficiency of PV systems and develop the reliability of PV generation control systems. In that manner, the comparison of overall technical and economic performance of different PV system architectures is becoming an issue. There are two ways to increase the efficiency of PV power generation. The first is to develop materials offering high conversion efficiency at low cost. On the other hand, the most important issue is to operate PV systems optimally for getting better efficiency [1].

Table 5
Comparison performance of string and central based MPPT under continuous shaded patterns.

PV array	Measurements	String based MPPT control						Central based MPPT	
		V_1 (V)	P_1 (W)	V_2 (V)	P_2 (W)	V_3 (V)	P_3 (W)	V_c (V)	P_c (W)
10 × 3	Ideal	164.05	203.16	88.99	228.11	145.77	216.22	112	568
	RBF	173.80	177.60	79.10	210.41	141.50	212.99	110	562
	Local maxima	164.05	203.16	171.29	150.34	164.89	214.01	178	310
15 × 3	Ideal	170.52	207.04	152.35	267.91	176.82	287.16	179	720
	RBF	165.40	204.50	150.50	267.42	170.20	280.63	175	714
	Local maxima	259.90	91.34	255.09	127.46	266.11	104.55	255	452
20 × 3	Ideal	182.34	270.77	177.54	253.33	184.50	320.07	255	792
	RBF	179.27	269.10	170.35	247.66	192.65	303.19	251	785
	Local maxima	338.03	130.77	325.40	127.58	342.95	171.93	352	525

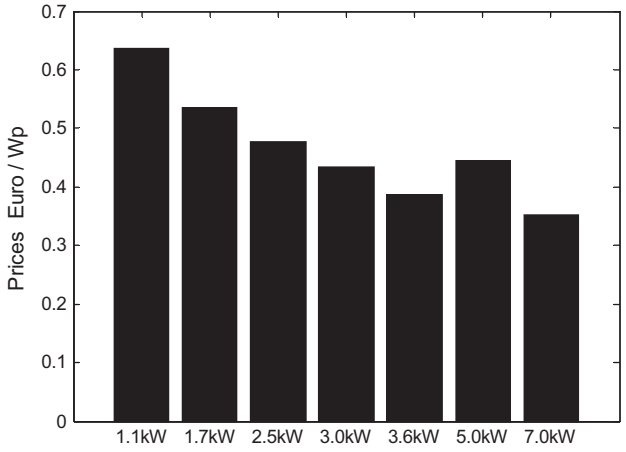

Fig. 8. Prices of PV Inverters.

The economic analysis is not yet sufficiently investigated due to the lack of detailed information about investment and field data of PV plants [15]. On the other hand, the comparison results strongly depend on unpredictable factors such as the amount of solar radiation, clouds, shadows, dirt or other obstructions that effect the amount of power generated. He et al. proposed a method to evaluate the impact of inverter configuration on energy cost of grid-connected PV systems under the assumption that uniform operation conditions are ensured and partial shading conditions are avoided during the design and constructions of PV plants [15]. Cellura et al. proposed a methodology for assessing energy and economic performances of PV systems in a large urban context [48]. The case study showed that the shading effects due to the surrounding obstacles and the incentives play important roles in the diffusion of the PV systems [48]. In that manner, PV companies have started to use the terms of levelized cost of energy (LCE) that is one of the commonly used indicators in order to enable comparisons between alternative energy technologies [49]. Mediavilla et al. studied the importance of an appropriate choice of elements for the installation [50]. They showed that the homogeneity of the characteristic curves of the panels in use appears to be an indicator of system quality.

Three factors can be categorized when comparing performance of different PV system configurations: capital costs, energy harvesting, and maintenance. The capital cost includes PV modules, power electronic equipments, and installation costs. For residential and commercial installations, the inverter will typically be rated at between 1 kWp and 7 kWp. The inverters will cost around €0.35–0.65 per Wp (Fig. 8) [48]. The inverter price (€/Wp) decreases with inverter's rated capacity. The total investment costs of PV inverters can be calculated by multiplying the nominal power of the inverter with the specific investment costs of the inverter (€/Wp). If a PV module price is €2 [48] per Wp, the module cost for a 3.3 kWp system therefore is €6600. Fig. 9 presents the contributing components to the total capital cost of the three strings and central based PV system. The mounting, cabling, connectors, and main switchboard costs can also form the third major contributor to the total capital cost. For string based topology, as the number of inverters increases, the contribution of inverters to the total capital cost of PV system also increases. However, the analysis shows that PV

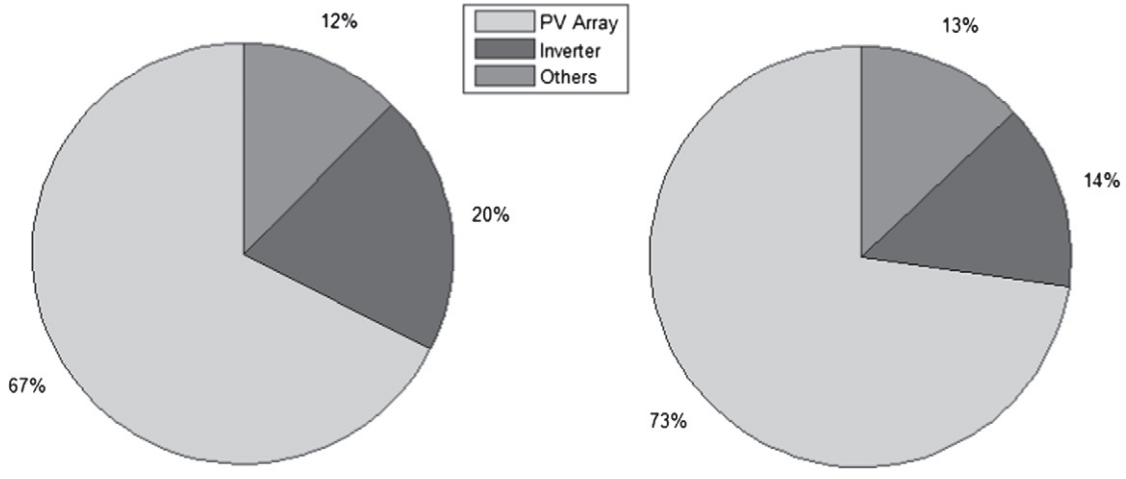

(a) String inverter based topology (b) Central inverter based topology

Fig. 9. Cost distribution of a 3.3 kWp PV installation.

array plays as a first major contributor for both cases. A similar result was obtained for PV remote area power systems in [51].

Table 4 shows the benefit of the proposed method in terms of the total power harvested of PV systems under the partial shading conditions. The incremental output power is in the range between 28.43% and 62.73% for both topologies. When considering the minimum average contribution (28.43%), the proposed method offers a €1848 advantage. If the power difference between the local and global MPP is higher and the non-uniform operating conditions continue for longer duration, there will be significant increase in the extracted power and energy in the proposed method in both string and central topologies. As a result, PV system with the proposed method can provide a considerable amount of electricity, making a significant contribution to payback period of PV systems [52]. The main benefit of the proposed method is that mismatch power loss can be reduced significantly for both topologies.

6. Conclusion

A new method for maximum power point tracking of photovoltaic arrays under various non-uniform irradiance conditions which can reduce mismatching losses significantly with respect to the conventional method has been developed. Under this condition, it is well-known that there are certain numbers of multiple peaks as the number of PV modules in one-string increases due to the nature behavior of bypass diode. Since the conventional control method is only operating the PV system at the local maxima close to open circuit voltage, only small portion of power can be extracted from the PV system. Therefore, the radial basis function artificial neural network based intelligent control method is utilized to identify the global operating voltage on each string of PV array. The proposed method is well-recognizable fast during the training process, the network structure is directly confirmed after training and it has high accuracy during the validation. Also it has the flexibility to deal with different size of PV array because only retraining process is necessary and this process is fast. The proposed method is compared with the ideal case and conventional method through observing the power–voltage curve of PV arrays. The proposed method has been tested in 10×3 (2.2 kW), 15×3 (2.5 kW) and 20×3 (3.3 kW) of series–parallel (SP) PV array configuration under random-shaded and continuous-shaded patterns. The simulation results show that under randomly shaded pattern, there are significant increases of about 30–60% of the extracted power in one operating condition. This is also observed in the continuous shading pattern where the proposed controller is able to shift the operating voltage on each string module to their optimum voltages.

References

[1] Karatepe E, Hiyama T, Boztepe M, Colak M. Voltage based compensation system for PV generation system under partially shaded insolation conditions. Energ Convers Manage 2008;49:2307–16.

[2] Guangyu L, Nguang SK, Partridge A. A general modeling method for *I–V* characteristics of geometrically and electrically configured photovoltaic arrays. Energ Convers Manage 2011;52:3439–45.

[3] Ubisse A, Sebitosi A. A new topology to mitigate the effect of shading for small photovoltaic installations in rural sub-Saharan Africa. Energ Convers Manage 2009;50:1797–801.

[4] Kaushika ND, Rai AK. An investigation of mismatch losses in solar photovoltaic cell networks. Energy 2007;32:755–9.

[5] Van der Borg N.J.C.M, Jansen M.J. Energy loss due to shading in BIPV application. In: Proceeding of the 3rd world conference on photovoltaic energy conversion, Osaka (Japan), May 2008. p. 2220–2222.

[6] Liu B, Duan S, Cai T. Modeling and coordinate control of photovoltaic DC building module based BIPV system. Sol Energy 2012;86:482–8.

[7] Yoon JH, Song J, Lee SJ. Practical application of building integrated photovoltaic (BIPV) system using transparent amorphous silicon thin-film PV module. Sol Energy 2011;85:723–33.

[8] Chouder A, Silvestre S. Automatic supervision and fault detection of PV systems based on power losses analysis. Energ Convers Manage 2010;51:1929–37.

[9] Salas V, Olías E. Overview of the state of technique for PV inverters used in low voltage grid-connected PV systems: Inverters below 10 kW. Renew Sust Energ Rev 2009;13:1541–50.

[10] Marańda W, Mey GD, Vos AD. Optimization of the master–slave inverter system for grid–connected photovoltaic plants. Energ Convers Manage 1998;39:1239–46.

[11] Mohd A, Ortjohann E, Morton D, Omari O. Review of control techniques for inverters parallel operation. Electr Pow Syst Res 2010;80:1477–87.

[12] Mellit A, Pavan AM. Performance prediction of 20 kW_p grid-connected photovoltaic plant at Trieste (Italy) using artificial neural network. Energ Convers Manage 2010;51:2431–41.

[13] Henze N, Sahan B, Burger R, Belschner W. A. Novel AC module with high-voltage panels in CIS technology. In: Proceeding of the 23rd European PV solar energy conference and exhibition, Valencia (Spain), September 2008.

[14] Shimizu T, Hirakata M, Kamezawa T, Watanabe H. Generation control circuit for photovoltaic modules. IEEE T Power Electr 2001;16:293–300.

[15] He F, Zhao Z, Yuan L. Impact of inverter configuration on energy cost of grid-connected photovoltaic systems. Renew Energ 2012;41:328–35.

[16] El-Dein M.Z.S, Kazerani M, Salama M.M.A. Novel configurations for photovoltaic farms to reduce partial shading losses. In: Proceeding of 2011 IEEE power and energy society general meeting, San Diego, CA, 24–29 July 2011. p. 1–5.

[17] Villarejo J.A, Molina-Garcia A, De Jodar E. Comparison of central –vs- distributed inverters: application to photovoltaic systems. In: Proceeding of 2011 IEEE international symposium on industrial electronics (ISIE), Gdansk, 27–30 June 2011.

[18] Deline C. Partially shaded operation of multi-string photovoltaic systems. In: Proceeding of 2010 IEEE 35th photovoltaic specialists conference (PVSC), Honolulu, HI, 20–25 June 2010.

[19] Anssi M, Seppo V. Power losses in long string and parallel-connected short strings of series-connected silicon-based photovoltaic modules due to partial shading conditions. IEEE T Energy Conver 2012;27:173–83.

[20] Foiadelli F, Leva S, Zaninelli D. PQ and protection system analysis of a new topology for grid connected PV Plant. In: Proceeding of international conference on clean electrical power (ICCEP), Ischia, 14–16 June 2011.

[21] Garcia M, Maruri JM, Marroyo L, Lorenzo E, Perez M. Partial shadowing, MPPT performance and inverter configurations: Observations at tracking PV plants. Prog Photovoltaics Res Appl 2008;16:529–36.

[22] James PAB, Bahaj AS, Braid RM. PV array < 5 kW + single inverter = grid connected PV system: are multiple inverter alternatives economic. Sol Energy 2006;80:1179–88.

[23] Zhang X, Ni H, Yao D, Cao R.X, Shen W.X. Design of single phase grid-connected photovoltaic power plant based on string inverters. In: Proceeding of 1st IEEE conference on industrial electronics and application, Singapore, May 2006. p. 1–5.

[24] Demoulias C. A new simple analytical method for calculating the optimum inverter size in grid-connected PV plants. Electr Pow Syst Res 2010;80:1197–204.

[25] Luoma J, Kleissl J, Murray K. Optimal inverter sizing considering cloud enhancement. Sol Energy 2012;86:421–9.

[26] Notton G, Lazarov V, Stoyanov L. Optimal sizing of a grid-connected PV system for various PV module technologies and inclinations, inverter efficiency characteristics and locations. Renew Energ 2010;35:541–54.

[27] Salas V, Alonso-Abellá M, Chenlo F, Olías E. Analysis of the maximum power point tracking in the photovoltaic grid inverters of 5 kW. Renew Energ 2009;34:2366–72.

[28] Syafaruddin, Karatepe E, Hiyama T. Polar coordinated fuzzy controller based real-time maximum-power point control of photovoltaic system. Renew Energ 2009;34:2597–606.

[29] Karatepe E, Syafaruddin, Hiyama T. Simple and high efficiency photovoltaic system under non-uniform operating conditions. IET Renew Pow Gener 2010;4:354–69.

[30] Erickson RW, Maksimovis D. Fundamentals of power electronics. Kluwer Academic Publishers; 2004.

[31] Karatepe E, Boztepe M, Colak M. Development of a suitable model for characterizing photovoltaic arrays with shaded solar cells. Sol Energy 2007;81:977–92.

[32] Ishaque K, Salam Z, Taheri H. Simple, fast and accurate two-diode model for photovoltaic modules. Sol Energ Mat Sol C 2010;95:586–94.

[33] Karatepe E, Boztepe M, Colak M. Neural network based solar cell model. Energ Convers Manage 2006;47:1159–78.

[34] Nguyen TL, Low KS. A global maximum power point tracking scheme employing DIRECT Search Algorithm for photovoltaic systems. IEEE T Ind Electron 2010;57:3456–67.

[35] Messai A, Mellit A, Massi Pavan A, Guessoum A, Mekki H. FPGA-based implementation of a fuzzy controller (MPPT) for photovoltaic module. Energ Convers Manage 2011;52:2695–704.

[36] Esen H, Ozgen F, Esen M, Sengur A. Artificial neural network and wavelet neural network approaches for modelling of a solar air heater. Expert Syst Appl 2009;36:11240–8.

[37] Esen H, Inalli M, Sengur A, Esen M. Artificial neural networks and adaptive neuro-fuzzy assessments for ground-coupled heat pump system. Energ Buildings 2008;40:1074–83.

[38] Esen H, Inalli M, Sengur A, Esen M. Modelling a ground-coupled heat pump system by a support vector machines. Renew Energ 2008;33:1814–23.
[39] Sun X, Wu W, Li X, Zhao Q. A research on photovoltaic energy controlling system with maximum power point tracking. In: Proceeding of the power conversion conference PCC, Osaka (Japan), 2–5 April 2010, p. 822–826.
[40] Syafaruddin, Karatepe E, Hiyama T. Artificial neural network polar coordinated fuzzy controller based maximum power point tracking control under partially shaded conditions. IET Renew Pow Gener 2009;3:239–53.
[41] Torres A.M, Antunes F.L.M, Reis F.S. An artificial neural network-based real time maximum power tracking controller for connecting a PV system to the grid. In: Proceeding of the 24th annual conf. of the IEEE on industrial electronics society, vol. 1, p. 554–558.
[42] Esen H, Inalli M, Sengur A, Esen M. Predicting performance of a ground source heat pump system using fuzzy weighted pre-processing based ANFIS. Build Environ 2008;43:2178–87.
[43] Esen H, Inalli M, Sengur A, Esen M. Forecasting of a ground-coupled heat pump performance using neural networks with statistical data weighting pre-processing. Int J Therm Sci 2008;47:431–41.
[44] Reddy KS, Ranjan M. Solar resource estimation using artificial neural networks and comparison with other correlation models. Energ Convers Manage 2003;44:2519–30.
[45] Ashhab MSS. Optimization and modeling of a photovoltaic solar integrated system by neural networks. Energ Convers Manage 2008;49:3349–55.
[46] Esen H, Ozgen F, Esen M, Sengur A. Modelling of a new solar air heater through least-squares support vector machines. Expert Syst Appl 2009;36:10673–82.
[47] Mellit A, Menghanem M, Bendekhis M. Artificial neural network model for prediction solar radiation data: application for sizing standalone photovoltaic power system. In: Proceeding of IEEE Power Engineering Society General Meeting, vol. 1, 2005. p. 40–44.
[48] Cellura M, Gangi AD, Longo S, Orioli A. Photovoltaic electricity scenario analysis in urban contests: An Italian case study. Renew Sust Energ Rev 2012;16:2041–52.
[49] Mousazadeh H, Keyhani A, Javadi A, Mobli H, Abrinia K. Life-cycle assessment of a solar assist plug-in hybrid electric tractor (SAPHT) in comparison with a conventional tractor. Energ Convers Manage 2011;52:1700–10.
[50] Díez-Mediavilla M, Alonso-Tristán C, Rodríguez-Amigo MC, García-Calderón T, Dieste-Velasco MI. Performance analysis of PV plants: Optimization for improving profitability. Energ Convers Manage 2012;54:17–23.
[51] Enslin JHR, Wolf MS, Snyman DB, Swiegers W. Integrated Photovoltaic Maximum Power Point Tracking Converter. IEEE T Ind Electron 1997;44: 769–73.
[52] Al-Salaymeh A, Al-Hamamre Z, Sharaf F, Abdelkader MR. Technical and economical assessment of the utilization of photovoltaic systems in residential buildings: The case of Jordan. Energ Convers Manage 2010;51:1719–26.